Optical Engineering

OpticalEngineering.SPIEDigitalLibrary.org

High-bandwidth fine tracking system for optical communication with double closed-loop control method

Yukun Wang
Dayu Li
Rui Wang
Chengbin Jin
Shaoxin Wang
Quanquan Mu
Li Xuan
Zhaoliang Cao
Zhi Wang

SPIE.

Yukun Wang, Dayu Li, Rui Wang, Chengbin Jin, Shaoxin Wang, Quanquan Mu, Li Xuan, Zhaoliang Cao, Zhi Wang, "High-bandwidth fine tracking system for optical communication with double closed-loop control method," *Opt. Eng.* **58**(2), 026102 (2019), doi: 10.1117/1.OE.58.2.026102.

High-bandwidth fine tracking system for optical communication with double closed-loop control method

Yukun Wang,[a,b,†] Dayu Li,[a,†] Rui Wang,[a,b] Chengbin Jin,[a,b] Shaoxin Wang,[a] Quanquan Mu,[a] Li Xuan,[a] Zhaoliang Cao,[a] and Zhi Wang[a,*]

[a]Chinese Academy of Sciences, Changchun Institute of Optics, Fine Mechanics and Physics, State Key Laboratory of Applied Optics, Changchun, China

[b]University of Chinese Academy of Sciences, Beijing, China

Abstract. A fine tracking system is crucial for maintaining the accuracy of the optical communication terminals that aim at each other. To ensure the reliability of the communication link, the fine tracking system requires high bandwidth to mitigate the effect of arrival angle fluctuation caused by atmospheric turbulence. Traditionally, the fine tracking system includes only a single feedback loop; a high bandwidth is obtained by increasing the high gain of the fine tracking system, which usually suffers considerably from the time delay engendered by sampling and data processing, the hysteresis nonlinearity of a fast steering mirror (FSM), and the limitations of dynamic response of FSM. To track the beacon in real time and with high precision, a pioneering control method is presented in our paper, namely, double closed-loop control (DCC), which performs better in a tracking system compared with a traditional single-feedback loop. In the inner feedback loop, the response of FSM is measured by a strain gauge sensor (SGS) and used as the inner feedback signal. Thus, by co-operating with the outer CCD-based feedback loop, a DCC scheme is proposed for the fine tracking system. With the SGS signal, the inner loop controller is designed to obtain a rapid response without overshooting; meanwhile, the hysteresis nonlinearity is diminished. Experimental results indicate that the static hysteresis nonlinearity of FSM is reduced from 15.6% to 1.4% by an inner feedback loop, and the dynamic response and stability of FSM is greatly improved, thereby simplifying the outer loop controller design. Then, with the SGS signal, the time delay of the outer loop can be compensated accurately with a predicted signal compensation method. The experimental results show that the −3 dB error rejection bandwidth is increased from 76 to 85 Hz, and the coupling efficiency in our optical communication system is improved by 16.87% after using the DCC fine tracking method. These results indicate that the DCC method can effectively achieve the goal of fast and accurate tracking for optical communications systems. [DOI: 10.1117/1.OE.58.2.026102]

Keywords: fine tracking system; atmospheric correction; optical communication; control bandwidth.

Paper 181612 received Nov. 10, 2018; accepted for publication Jan. 16, 2019; published online Feb. 5, 2019.

1 Introduction

Free-space optical communication (FSOC) has many advantages compared with the traditional radio frequency communication; these advantages include high data rate, free-license spectrum, low-power consumption, and excellent security on Ref. 1. Given that FSOC systems usually have a narrow beam divergence angle, they are extremely sensitive to atmospheric turbulence and mechanical vibration. High-accuracy beacon-beam tracking is crucial in establishing and maintaining the communication links, which are essential in the success of the entire communication. Generally, the tracking bandwidth is directly determined by the performance of the fine tracking loop of an acquisition, tracking, and pointing system.[2] Therefore, the design of a high-bandwidth fine tracking control system is a very important element for the FSOC links.

Most fine tracking systems include only a single feedback control loop, and the most common control method is the simple and effective proportional integration differential (PID) control method.[3,4] To improve the bandwidth of the fine tracking system, some researchers increased the gain of the PID controller for higher bandwidth. However, a much higher gain easily leads to system instability.[5] Some researchers increase the correction frequency of the closed loop by decreasing the CCD exposure time. However, the signal-to-noise ratio is decreased, and the detection accuracy cannot be guaranteed. Thus, the exposure time of the CCD sensor must be sufficiently large to ensure the detection precision. When considering the CCD exposure time and data processing time, the time delay in the fine tracking control loop is a major problem that will seriously affect the tracking accuracy. To solve this problem, many control methods have been investigated to decrease the effect of the time delay. First, an atmospheric-turbulence-prediction-based control method is presented to compensate for time delay.[6,7] However, when the atmosphere turbulence becomes stronger, the prediction precision is low. Recently, a predicted signal compensation method (PSCM) has been proposed to compensate for time delay.[8] In this method, the prediction validity is sensitive to the accuracy of the fine tracking control system model. Furthermore, the inherent hysteresis nonlinearity and the dynamic response of the fast steering mirror (FSM) limit the bandwidth of the fine tracking system. Thus, satisfying the accuracy requirements of the fine tracking system for FSOC is difficult or even impossible.

*Address all correspondence to Zhi Wang, E-mail: wz070611@126.com

†These authors contributed equally to this work.

0091-3286/2019/$25.00 © 2019 SPIE

In this paper, a double closed-loop control (DCC) scheme is proposed for the fine tracking system. By co-operating with the original CCD-based outer feedback loop, an inner feedback loop is introduced to improve the inherent hysteresis nonlinearity and dynamic response of the FSM, in which a strain gauge sensor (SGS) is used to measure the FSM response signal with a sample rate of 10 kHz. The contribution of this SGS-based inner feedback loop is the hysteresis compensation and the optimization of dynamic response. Afterward, the overall inner loop can be considered a linear time-invariant system, and the dynamic response is fast and accurate, thereby contributing to the outer loop controller design and optimization. Furthermore, given the SGS signal, the identification of the fine tracking system model can be avoided. Thus, the time delay of the outer loop can be accurately compensated with the predicted signal compensation control method (PSCM).[8] Experimental results indicate that the controller algorithm is simple, highly stable, and accurate in solving the time delay and the inherent hysteresis nonlinearity problem. The dynamic response is improved considerably. Compared with the traditional PID and previous PSCM, the method has many advantages, such as better robustness, fewer demands on the system model, and better control effect.

2 Fine Tracking System Scheme

2.1 *Traditional CCD-Based Fine Tracking Scheme*

The scheme of a traditional fine tracking system is shown in Fig. 1. The fine tracking system is composed of CCD sensor, control computer (CC), digital-to-analog converter (DAC), high-voltage amplifier (HVA), and FSM. The fine tracking system includes only a single feedback loop. The residual aberration ϕ^{res} is detected by the CCD with detection noise n. The driving voltages for FSM are computed and sent to FSM by CC, DAC, and HVA. Then, the FSM correction ϕ^{cor} will compensate the tracking signal ϕ^{r} as feedback.

For the above control scheme, the most effective method used in improving the performance of the fine tracking system is to increase the gain of the controller for a high bandwidth, which, however, usually suffers considerably from a low CCD sampling rate and the mechanical limitations of FSM. Therefore, a tentative approach to the optimization of the control scheme with an inner feedback is proposed.

2.2 *Double Closed-Loop TT Control Scheme*

The diagram of the DCC fine tracing system is depicted in Fig. 2. An inner feedback control loop is introduced to compensate for hysteresis nonlinearity in the piezoelectric actuators and to improve the dynamic performance of the FSM response.

As shown in the dotted line of Fig. 2, the inner feedback loop consists of SGS, an ADC, and an inner controller (CC_{inner}). The SGS is a linear sensor, which has a high resolution of less than 1 μrad. The SGS transfers the response of FSM linearly to the corresponding voltage and it is fed back with a sample rate of 10 kHz. CC_{inner} is the inner SGS-based controller; it computes the driving voltages for FSM. The overall inner loop can be considered a whole. It is a linear system without hysteresis nonlinearity; the performance of the linear system can be optimized by the design of CC_{inner}. In Sec. 3, the CC_{inner} and CC_{outer} are designed to optimize the overall performance of the fine tracking system in detail.

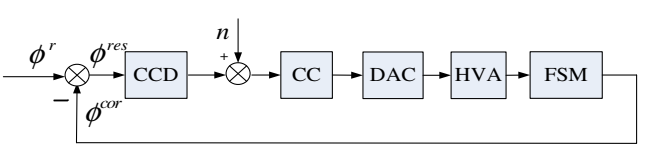

Fig. 1 Control scheme of the fine tracking system.

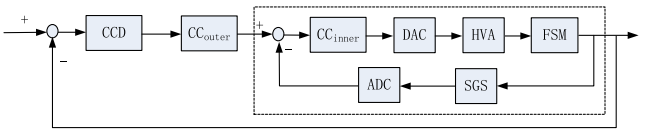

Fig. 2 Diagram of double closed-loop fine tracking control scheme.

3 Double Closed-Loop Controller Design

Based on the control scheme proposed in the previous section, the DCC is designed in two steps: the (1) inner SGS-based controller design and the (2) outer CCD-based controller design. To optimize the final performance of fine tracking, a time-delay compensation control method is designed with the SGS signal.

3.1 *Inner SGS-Based Controller Design*

The inner SGS-based position control loop diagram is shown in Fig. 3. The inner controller is a second order controller that aims at compensating the inherent hysteresis nonlinearity and improving the dynamic performance of FSM.

We choose a traditional second order system to describe the properties of the HVA and FSM that may be expressed as in Eq. (1):

$$G_p(s) = \frac{k}{s^2 + cs + p}, \tag{1}$$

where k, c, p are the parameters of the FSM system model; the parameters can be obtained by system identification methods. The transfer function of ADC and DAC can be described as follows:

$$G_{\text{ADC}}(s) = G_{\text{DAC}}(s) = \frac{1 - e^{-Ts}}{Ts} \approx e^{-Ts/2}, \tag{2}$$

where T is the sampling time. Thus, we can easily obtain the inner closed-loop transfer function $G_{\text{closed\_in}}$:

$$G_{\text{closed\_in}}(s) = \frac{G_{cc\_in}(s)G_p(s)}{1 + G_{cc\_in}(s)G_p(s)e^{-Ts}} e^{-Ts}. \tag{3}$$

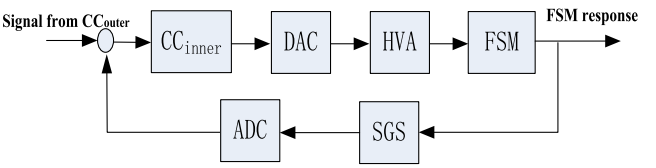

Fig. 3 Inner SGS-based position loop controller diagram.

A perfect inner controller can be designed as follows:

$$G_{cc\_in}(s) = \frac{k_c}{s} G_p^{-1}(s). \tag{4}$$

To simplify the expression, we use a first-order filter to approximate the time delay:

$$e^{-Ts} = \frac{1 - Ts/2}{1 + Ts/2} = \frac{a - s}{a + s}, \tag{5}$$

where $a = 2/T$, $G_{\text{closed\_in}}$ can be reduced to the following form:

$$\begin{aligned} G_{\text{closed\_in}}(s) &= \frac{k_c e^{-Ts}}{s + k_c e^{-Ts}} = \frac{k_c(a - s)}{s^2 + (a - k_c)s + ak_c} \\ &= \frac{k_c(a - s)}{s^2 + 2\xi_n \omega_n s + \omega_n^2}, \end{aligned} \tag{6}$$

where ω_n is the natural frequency and ξ_n is the damping coefficient. To obtain an optimal closed-loop system, the damping coefficient should satisfy

$$\xi_n = \sqrt{\frac{(a - k_c)^2}{4ak_c}} = \frac{\sqrt{2}}{2}. \tag{7}$$

Considering the stability of the system, the relationship between a and k_c should satisfy $k_c < a$. Then, we can easily obtain the following equation:

$$k_c = \frac{a}{2 + \sqrt{3}}. \tag{8}$$

With the optimal inner loop controller, the inherent hysteresis nonlinearity and dynamic performance of FSM can be improved as our design. Then, the outer loop controller can be designed based on the inner closed-loop system response.

3.2 *Outer CCD-Based Controller Design with PSCM*

The control scheme of an outer CCD-based controller with PSCM is shown in Fig. 4. $e(k)$ is the residual tracking aberration detected by the CCD sensor, with the detection noise n. Owing to the effect of the delay time τ, the FSM moves during the delay time. Then, the measured residual aberration $e(k)$ is not accurate. To overcome this problem, the PSCM is presented;[8] the principle of PSCM is to compensate the measuring aberration with the identified model $G_m(s)$ during the delay time. The driving voltage is calculated by taking the compensated aberration into the PID controller. $e'(k)$ is the residual with compensation, and $y(k)$ is the output of the identified model $G_m(s)$. It is used to calculate

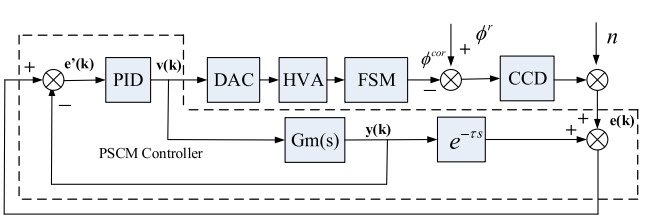

Fig. 4 Control scheme of the TT correction system.

$e'(k)$. With $e'(k)$, the driving voltages $v(k)$ can be computed accurately. Thus, the performance of PSCM is dependent on the accuracy of the identified model $G_m(s)$.

The mathematical expression of the PSCM controller can be described as in Eq. (9):

$$\begin{cases} v(k) = v(k-1) + k_1 e'(k) + k_2 e'(k-1) + k_3 e'(k-2) \\ e'(k) = e(k) + y(k) - y(k - nT) \end{cases}, \tag{9}$$

where, k_1, k_2, k_3 are the parameters of PID, and $y(k - nT)$ is the $G_m(s)$ with n steps delay. To avoid the identification of the system model, we use the SGS sensor to measure the FSM positions; the positions are recorded at the start and the end of CCD exposure. Thus, the $y(k)$ and $y(k - nT)$ in Eq. (9) is accurate. The mathematical expression of the PSCM controller can be changed to

$$\begin{cases} v(k) = v(k-1) + k_1 e'(k) + k_2 e'(k-1) + k_3 e'(k-2) \\ e'(k) = e(k) + k_{sgsTocd}(y_{sgs}(k) - y_{sgs}(k - nT)) \end{cases}, \tag{10}$$

where $y_{sgs}(k)$ nd $y_{sgs}(k - nT)$ are the SGS signal at the start and the end of CCD exposure. $k_{sgsTocd}$ is a parameter for converting SGS signal value in accordance with the CCD signal value. This parameter can be measured in advance.

In this control scheme, we optimize the inner loop first. The inherent hysteresis nonlinearity and dynamic response are optimal; this situation is helpful for the design of the outer PID controller. Meanwhile, the SGS sensor is used to compensate the time delay with PSCM; the compensation accuracy can be improved considerably compared with the traditional single-loop PSCM.

4 Experiment and Results

In our system, a PI S330.2SL high-dynamics piezo FSM platform is used. A CCD camera with the fastest sampling frequency of 1.67 kHz is used as the fine tracking detector. Our experiment is conducted based on these factors to test the DCC method. The SGS-based FSM model is identified, and the optimal inner controller is first obtained with the previous design. The performance of the inner SGS-based controller is tested by a laboratory experiment. Then, the outer CCD-based controller with PSCM is designed for this experimental system. The bandwidth of our fine tracking system is measured and compared with our previous methods. Finally, this system is installed in our optical communication system, and the performance of optical communication is analyzed after using the DCC method.

4.1 *Experiment Setup for the Design of Inner SGS-Based Controller*

The components in the inner control loop are a PI S330 FSM with SGS, NI PCIe6251 card for SGS data acquisition and sending of driving voltages, and a computer for data processing and controller realization. The experimental platform for the inner loop design is shown in Fig. 5. The PI S330 FSM is the gray box in Fig. 5, which consists of an SGS sensor module and a high-voltage driving module. The NI PCIe6251 card is the white interface box in Fig. 5, which consists of 2 channels of analog voltage output and 16 channels of

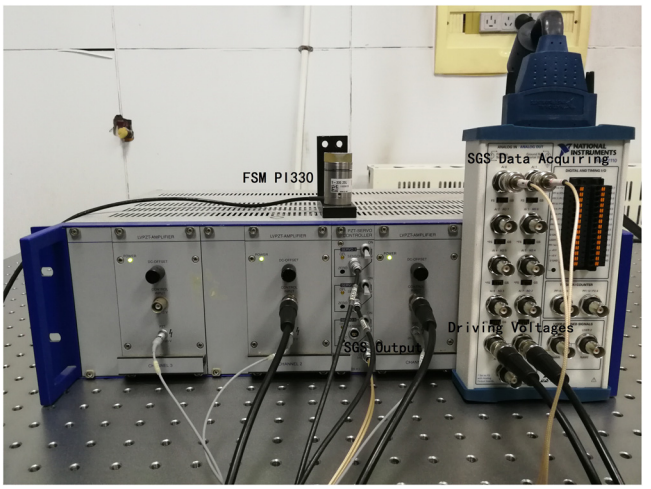

Fig. 5 Experimental platform for inner loop design.

analog data acquisition, it satisfies the experimental requirements. The SGS-based FSM model is identified with the method mentioned in Ref. 9. The sampling time of the NI PCIe6251 card is ∼0.1 ms; thus, $T = 0.1$ ms in our system. Considering the limitation of the dynamic range of FSM and the driving voltage range of NI PCIe6251 card, the control parameter k_c is limited. The inner loop controller is a suboptimal control.

To verify the inner control loop performance, the frequency response is measured from 5 to 495 Hz. Then, we can design the inner controller with the response and measure the frequency response of the inner closed loop. The results are shown in Fig. 6.

As shown in Fig. 6, the red line is the frequency response of the inner closed loop, whereas the blue line is of the original nonlinear response. The amplitude of the open loop FSM is −2 dB at low frequency and begins to decrease at a middle frequency of ∼90 Hz. The open loop cut-off frequency is considered as 300 Hz, and the phase lag is ∼60 deg. After inner closed-loop correction, the amplitude of the closed loop frequency response is 0 dB at low frequency and begins to decrease at ∼180 Hz. The phase lag is

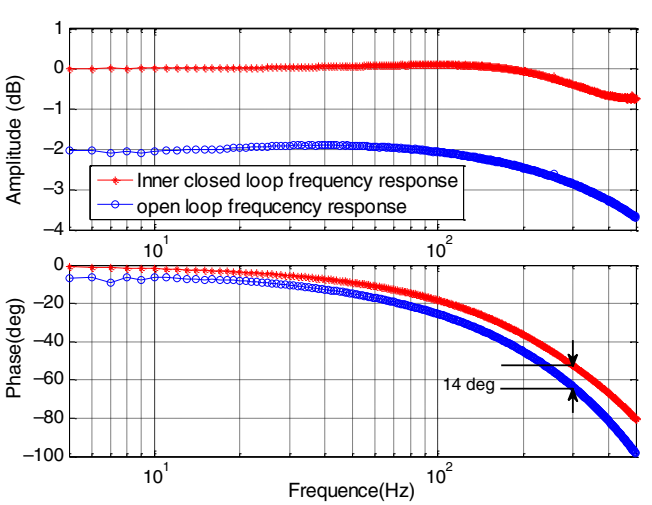

Fig. 6 Frequency response curves of the FSM platform (a) with and (b) without an inner closed loop.

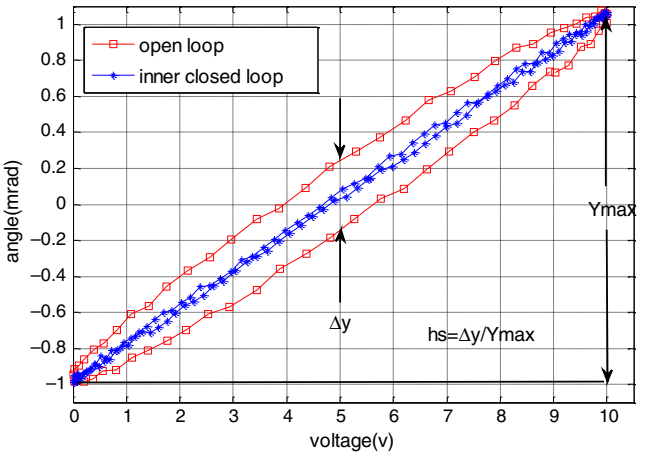

Fig. 7 Hysteresis curves with and without an inner closed loop.

46 deg. The results show that after the inner closed loop, the response is stable and accurate. The bandwidth is increased by ∼90 Hz and the phase lag is decreased by 14 Hz; the dynamic response linearity of the FSM is improved greatly. Then, the inherent hysteresis curves of FSM are measured, and the result is shown in Fig. 7.

To quantify the hysteresis nonlinearity, we define hs as the ratio of the maximum possible output difference for any input (Δy) divided by the output range ($Y_{\max}$), $hs = \Delta y / Y_{\max}$ (Fig. 7). As shown in Fig. 7, the hysteresis parameter hs has been reduced from 15.6% to 1.4% by an inner closed loop, and the linearity of the input–output curve has been improved greatly.

4.2 *Performance of Double Closed-Loop Control*

After the design of the inner closed loop, the inner loop can be considered an integrity. The response of the inner closed loop is a linear system with good dynamic characteristics. The outer loop controller can be effectively designed with SGS time delay compensation. The purpose of the control system is to improve the bandwidth of a fine tracking system. Thus, we compare the −3 dB error rejection bandwidth between the traditional single-loop PSCM and the control SGS time delay compensation method proposed in this paper.

In traditional single loop PSCM controller design, owing to the system hysteresis nonlinearity, the accurate dynamic model of the FSM platform is not available and the controller parameters cannot be directly optimized. Thus, the trial and error method is used in determining the parameters. When an inner SGS-based inner closed loop is introduced, the FSM platform is almost linearized with a good dynamic response. To verify the fine tracking performance, we established an experimental platform for measuring the bandwidth of the fine tracking system. The optical layout is shown in Fig. 8. FSM1 and FSM2 are conjugated with each other. The light outputted with a fiber bundle (diameter = 200 μm, wavelength is 400 to 700 nm) was collimated by lens L1 ($f = 80$ mm); the light diameter is limited at 7.8 mm with an iris aperture and then reflected by the FSM1. The reflected light is zoomed out by the combination of L2 ($f = 100$ mm) and L3 ($f = 73$ mm) and then reflected by FSM2 and detected by the CCD after L4($f = 100$ mm). In this experimental system, the FSM1 (PI S334) is added

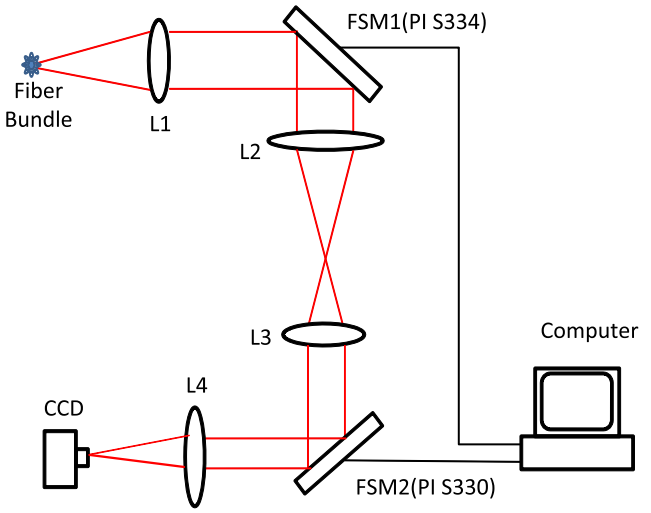

Fig. 8 Optical layout for bandwidth measuring of fine tracking system.

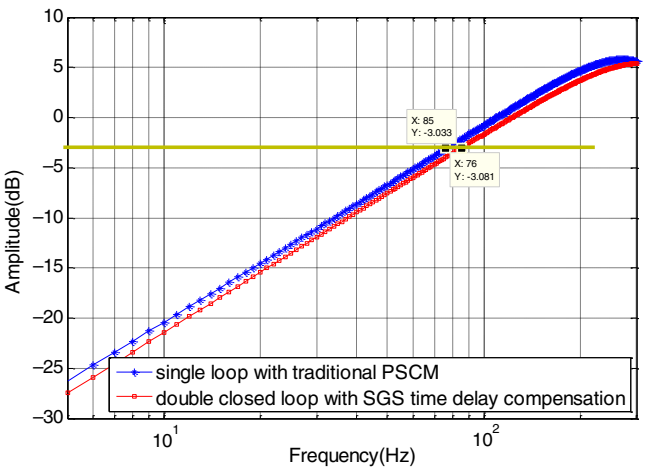

Fig. 9 Frequency response comparison of error rejection function.

Fig. 10 Optical layout of FSOC with disturbance FSM.

for generating the incoming disturbances, and the FSM2 (PI S330) is used as the corrector.

The frequency response curves of error rejection function are shown in Fig. 9. As shown in the figure, the precision of FSM is increased considerably and the time delay error is compensated accurately with SGS. The −3 dB error rejection bandwidth of the fine tracking control system increases from 76 to 85 Hz with our method.

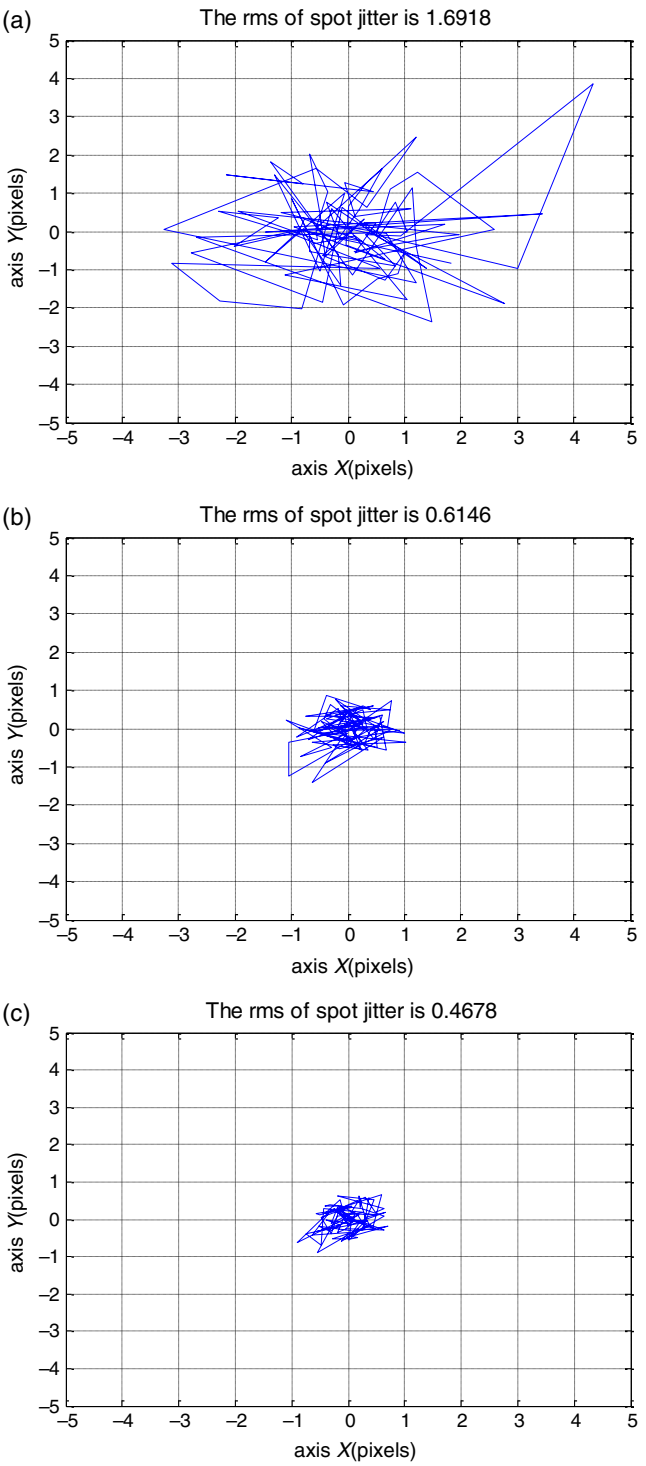

Fig. 11 Fine tracking results of FSOC: (a) uncorrected center of the light spot, (b) corrected center of the light spot with PSCM, and (c) corrected center of the light spot with DCC method.

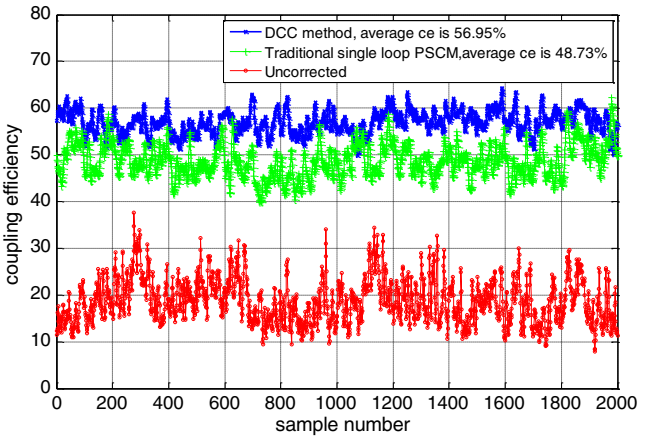

Fig. 12 CE after correction with PSCM and DCC method.

To verify the control performance in fine tracking, we examined this method in our FSOC. The detailed optical layout description of our FSOC is provided in Ref. 10. We add an FSM to generate disturbances in the FSOC; the label is FSM1 in FSOC. FSM1 and FSM2 are conjugated with each other. The data for FSM1 are collected from an 8.9-km terrestrial optical communication link by a CCD camera on November 27, 2017, at Dalian. In a laboratory, FSM1 is used to simulate the same CCD light spot as the outfield experiment. The Tylor frequency is 18 Hz. Then, we conducted a fine tracking experiment to verify our method. Figure 10 shows the optical layout of our FSOC with disturbance FSM.

The disturbance is generated by FSM1 and the data on disturbance were collected on CCD. First, the correction FSM is not accurate, and then the disturbance is corrected with the traditional single loop PSCM and DCC method, respectively. The residual disturbance data are collected on CCD. The results are shown in Fig. 11.

The results show that the RMS error of residual disturbance on CCD had been reduced by 23.89% on average compared with a traditional single loop PSCM. Then, we use coupling efficiency (CE) to evaluate the communication performance; the CE can be calculated by Eq. (11) as follows:[11,12]

$$\eta = \frac{8}{\pi^2 D^2 w_\alpha^2}|a|^2, \tag{11}$$

where

$$a = \iint_S \exp(-\frac{x^2 + \quad y^2}{w_\alpha^2})\cos[\varphi(x,y)]ds - j\iint_S \exp(-\frac{x^2+y^2}{w_\alpha^2})[\varphi(x,y)]\mathrm{d}s,$$

w_α is the radius of the optical fiber mode field, and φ is the wavefront residual aberration measured by WFS. Figure 12 shows the results of CE. The CE after correction with the DCC method is increased by 16.87% compared with the traditional single loop PSCM.

As bit error rate is the final standard for FSOC system, the bit error rate is calculated in this paper. As is shown in Fig. 12, the power entering the coupling fiber is increased with DCC method, the CE is increased from 48.73% to 56.95%. If the power in the whole pupil surface is 10 μW, the power entering the fiber is from 4.8 to 5.7 μW, with the formula in Ref. 11, the bit error rate is decreased from 2.7×10^{-7} to 3.6×10^{-9}, it is reduced by 2 orders of magnitude, hence, the improvement for FSOC is very significant. Meanwhile, the cost of DCC method is very small, only a SGS senor is added compared with traditional method. Therefore, the DCC method is very effective and easy to popularize, and has good application value.

5 Conclusion

In this paper, we presented a DCC scheme for the fine tracking control system in our FSOC. The inner SGS-based position control loop aimed at improving the inherent hysteresis nonlinearity and dynamic response of the FSM, whereas the outer CCD-based tracking loop used the SGS data to compensate for the time delay. The experiment results are highly encouraging, thereby indicating that after the inner closed loop, the hysteresis nonlinearity of FSM platform decreased from 15.6% to 1.4%, and the system −3 dB error rejection bandwidth of our DCC method has improved from 76 to 85 Hz compared with the traditional single-loop PSCM. Finally, the performance of our method in FSOC is experimentally verified. The RMS error of residual disturbance on CCD was reduced by 23.89% on average compared with the traditional single-loop PSCM and the CE is improved from 48.53% to 56.95%. These results are very important for communication link stability. Furthermore, the linearization of the nonlinear FSM platform is useful for the system simulation; controller optimization and that for other sophisticated controllers is possible. All of these effects will lead to the performance improvement of the fine tracking system.

Acknowledgments

This work was supported by the National Natural Science Foundation of China under Grant Nos. 61475152, 61378075, 61405194, and 61377032.

References

1. X. Yin et al., "Evaluation of the communication quality of free-space laser communication based on the power-in-the-bucket method," *Appl. Opt.* **57**(4), 573–581 (2018).
2. J. Wang et al., "Free-space laser communication system with rapid acquisition based on astronomical telescopes," *Opt. Express* **23**(16), 20655–20667 (2015).
3. Y. Zhang and G. Shijie, "High precision pointing and tracking technology for space optical communication," in *Asia Commun. and Photonics Conf.*, Optical Society of America, p. ATh3A.183 (2014).
4. E. Fedrigo, R. Muradore, and D. Zilio, "High performance adaptive optics system with fine tip/tilt control," *Control Eng. Pract.* **17**, 122–135, (2009).
5. T. Tang et al., "Acceleration feedback of a CCD-based tracking loop for fast steering mirror," *Opt. Eng.* **48**, 013001 (2009).
6. Q. Fu et al., "Experimental study on modified linear quadratic Gaussian control for adaptive optics," *Appl. Opt.* **53**(8), 1610–1619 (2014).
7. Y. Wang et al., "Adaptive inverse control for tip/tilt mirror in adaptive optics system," *Opt. Precis. Eng.* **23**(8), 2003–2010 (2015).
8. C. Wang et al., "Time delay compensation method for tip-tilt control in adaptive optics system," *Appl. Opt.* **54**(11), 3383–3388 (2015).
9. Y. Wang et al., "High-precision identification of a tip-tilt control system for the compensation of time delay," *Appl. Opt.* **56**(5), 1431–1437 (2017).
10. R. Wang et al., "Demonstration of horizontal free-space laser communication with the effect of the bandwidth of adaptive optics system," *Opt. Commun.* **431**, 167–173 (2019).
11. Y. Wang et al., "Performance analysis of an adaptive optics system for free space optics communication through atmospheric turbulence," *Sci. Rep.* **8**, 1124 (2018).

12. Y. M. Sabry et al., "Silicon micromirrors with three-dimensional curvature enabling lensless efficient coupling of free-space light," *Light Sci. Appl.* **2**, e94 (2013).

Yukun Wang obtained his master's degree from Beijing University of Aeronautics and Astronautics in 2013. He is now a researcher of Changchun Institute of Optics, Precision Machinery and Physics, Chinese Academy of Sciences. He mainly studies automatic control in adaptive optics systems.

Dayu Li is an associate researcher and master's supervisor of optical engineering. He graduated from Changchun Institute of Optical Precision Machinery and Physics, Chinese Academy of Sciences, in 2007 with a PhD degree. He mainly studied adaptive optics and GPU acceleration technology for wavefront reconstruction.

Rui Wang is a doctoral candidate of Changchun Institute of Optical Precision Machinery and Physics, Chinese Academy of Sciences. She mainly studies adaptive optics and laser communication technology.

Chengbin Jin is a PhD candidate of Changchun Institute of Optical Precision Machinery and Physics, Chinese Academy of Sciences, majoring in adaptive optics and laser communication technology.

Shaoxin Wang is a PhD candidate of Changchun Institute of Optical Precision Machinery and Physics, Chinese Academy of Sciences, majoring in adaptive optics and laser communication technology.

Quanquan Mu is a PhD supervisor and researcher at Changchun Institute of Optical Precision Machinery and Physics, Chinese Academy of Sciences, and mainly studies adaptive optics technology.

Li Xuan is a researcher and doctoral supervisor. He obtained his bachelor's degree in Jilin University in 1983, master's degree in Changchun Institute of Physics, Chinese Academy of Sciences in 1986, and PhD degree in engineering, Northeast University of Japan in 1998, and was selected into the Chinese Academy of Sciences/100-person Program in 1999, mainly engaged in liquid crystal adaptive optics, liquid crystal optical devices, and liquid crystal high scores.

Zhaoliang Cao is a researcher and doctor, graduated from Changchun Institute of Optics, Precision Machinery and Physics, Chinese Academy of Sciences, with a PhD degree in 2008. He is now the director of the Research Laboratory of Liquid Crystal Optics and Adaptive Optics, Changchun Institute of Optics and Machinery, Chinese Academy of Sciences.

Zhi Wang is a researcher at Changchun Institute of Optical Precision Machinery and Physics, Chinese Academy of Sciences, mainly engaged in mechanical structure design research.